THE ASTROPHYSICAL JOURNAL, 343:158–168, 1989 August 1

NEAR-INFRARED IMAGES OF NGC 1068: BAR-DRIVEN STAR FORMATION AND THE CIRCUMNUCLEAR COMPOSITION

HARLEY A. THRONSON, JR.,[1] MARK HERELD,[2] STEVEN MAJEWSKI,[3] MATTHEW GREENHOUSE,[1] PAUL JOHNSON,[1] EARL SPILLAR,[1] C. E. WOODWARD,[1] D. A. HARPER,[3] AND BERNARD J. RAUSCHER[3]

Received 1988 October 3; accepted 1989 January 18

ABSTRACT

Images of the inner 1'.5 (7.9 kpc) of the Seyfert galaxy NGC 1068 at H (1.6 μm) and K (2.2 μm) both show an impressive stellar bar not found by shorter visual wavelength observations. We discuss a pair of reasons why the core of this galaxy appears so different over a pair of wavelength regimes that are both dominated by stellar photospheric emission: substantial stellar population variations with position or the effects of dust obscuration or both. Due to the close spatial proximity between the bar, the bright mid-infrared dust emission, and the $J = 1 \rightarrow 0$ CO emission, the bar is likely to be directly responsible for confining the molecular gas, leading to extremely active star formation in a partial ring that surrounds the central disk. There may be little star formation within the bar itself, and the visual and near-infrared colors of the bar/disk region indicate that our images are dominated by emission from photospheres of evolved late-type giant or asymptotic giant branch stars, modified by the effects of dust both in absorption and in emission. The ring of near-infrared emission that surrounds the bar, as well as the spiral arms, are bright at K, probably due either to emission from warm dust or from newly formed supergiant stars. We estimate the mass of the central disk and bar of the galaxy and find $M_{\rm core} = 2\text{–}3 \times 10^{10}\ M_\odot$, within a radius of about 15″ (1.3 kpc) of the center. We conclude that the high current rate of star formation, about 100 $M_\odot$ yr^{-1}, is due primarily to a large mass of molecular gas, rather than an extremely efficient mechanism of stellar birth.

Subject headings: galaxies: individual (NGC 1068) — galaxies: stellar content — stars: formation

I. THE GALAXY

NGC 1068 (M77, 3C 71, Arp 37), the nearest Seyfert 2 galaxy, has been a popular target for astronomers since Fath (1909) argued that this object should be included in the class of "spiral nebulae" and interpreted its nuclear spectrum as the product of a mixture of hot gas and extremely distant stars. The galaxy is characterized by one of the brightest and most luminous circumnuclear disks yet studied. Out to a radius of about 1 kpc from the energetic nucleus (1 kpc = 11″.5 at the galaxian distance of 18.1 Mpc), emission from this disk is generally thought to be the consequence of recent, very active star formation. Mid- and far-infrared emission has been found to be concentrated in the Seyfert nucleus and surrounding $\sim 1'$ diameter region (Telesco *et al.* 1984; Tresch-Fienberg *et al.* 1987; Lester *et al.* 1987), as has another product of active star formation, visual line emission (Balick and Heckman 1985; Atherton, Reay, and Taylor 1985; Baldwin, Wilson, and Whittle 1987; Pogge 1988; Young, Kleinmann, and Allen 1988). Recently, Myers and Scoville (1987) mapped the $J = 1 \rightarrow 0$ CO emission, a tracer of molecular gas, and found it distributed in a pair of truncated spiral arms surrounding the bright core region. As Myers and Scoville note, interferometric observations are not sensitive to the lower spatial frequencies, which may explain some of the differences between their map and that of Kaneko *et al.* (1988), who report a different distribution of CO emission based on single-dish observations with the Nobeyama millimeter-wave telescope. For the purposes of our study, it suffices to note that the CO maps from both groups show local maxima in the molecular emission to lie outside the immediate vicinity of the nucleus of NGC 1068, at a radius of about 15″. Carbon monoxide emission within this radius is very modest or nonexistent.

Young, luminous stars heat dusty material from which they were formed. In a recent paper, Telesco and Decher (1988) find that the 10 μm emission from the warm dust approximately follows the distribution of CO line emission in this galaxy. In other words, a large fraction of the mid-infrared, CO, and visual line emission appears localized within a coarse annulus, surrounding the nucleus at a distance of about 15″ (1.3 kpc). Detailed discussion of the relative spatial positions of these outlying components can be found in Telesco and Decher and in Kaneko *et al.* This partial ring of mid-infrared and visual emission, mixed within the molecular gas, motivated us to seek the underlying stellar structure using near-infrared imaging.

Active star formation in NGC 1068 has apparently created a significant population of hot young stars that dominate the ultraviolet and visible light (see, e.g., Keel and Weedman 1978; Weedman and Huenemoerder 1985; Ichikawa *et al.* 1987). However, the abundant lower mass, cool evolved stars should dominate the emission from a wide variety of galaxies at very red and near-infrared wavelength (see, e.g., Frogel 1985 and references therein). To determine the distribution of these stars, we therefore imaged the H (1.6 μm) and K (2.2 μm) continuum emission from the central regions of NGC 1068. In our discussion, we compare our data with a number of other maps of the inner few arcminutes of the galaxy, including the recent work of Scoville *et al.* (1988), who used single-aperture mapping to study NGC 1068 at K and discovered a strong bar that is not apparent at shorter visual wavelengths (also, G. Bothun 1988, private communication). This situation is reminiscent of the result for the face-on spiral NGC 1566 several years ago when Hackwell and Schweizer (1983) found a distinct bar from their near-infrared observations in a galaxy that had only shown a faint bar at visual wavelengths. As part of

[1] Wyoming Infrared Observatory, University of Wyoming.
[2] Department of Astronomy and Astrophysics, University of Chicago.
[3] Yerkes Observatory, University of Chicago.

our analysis, we shall argue that galaxies with stellar bars that are visible only at near-infrared wavelengths may be fundamentally different from the well-known visual barred spirals.

II. THE OBSERVATIONS AND DATA REDUCTION

Near-infrared images of NGC 1068 were obtained with the Astrophysical Research Consortium (ARC) prototype near-infrared HgCdTe imaging camera (Hereld, Harper, and Pernic 1989) at the Cassegrain focus of the 2.3 m Wyoming Infrared Observatory (WIRO) telescope. Most of the data were obtained on the nights of 1987 September 10–12, during conditions of good seeing (0".5–1".5 arcsec) and moderate or good transparency. The camera was configured to give a scale of 0".59 pixel^{-1} with the f/27 beam of the telescope, producing net angular resolutions of 1"–1".5. The total field of view of the 64 × 64 array was 37".5 × 37".5. Exposure times were chosen so that the sky background was about half-well potential to ensure that object photons occupied the linear regime of the detector. Individual frames were 4 minutes in duration in the K band and 6 minutes in the H band, and each on-source observation was interleaved with a "sky" observation of equal integration time to correct for the changing characteristics of the night sky. Each reference position was about 3′ away from the region in the galaxy that we mapped. This position was within the optical extent of NGC 1068, but in a region whose near-infrared emission was much below that of the core.

We mapped the galaxy each night, beginning with an initial exposure of the center, followed by a series of frames offset by approximately 20". Each individual exposure therefore overlapped with an adjacent frame by about 50% to increase the signal-to-noise ratio and to ensure accurate image reconstruction. At intervals of about 20 minutes, a short exposure of a nearby SAO star was obtained to monitor sky conditions and telescope drift. The latter was found to be less than 0".2 per minute of time.

We processed the images by first subtracting an appropriate frame of blank sky, which, in most cases, was the weighted average of up to four sky exposures taken close in time to the object image. We intend this average sky image to be the most representative of the conditions during the period we were observing the source, while reducing the contribution of the sky subtraction to the noise in our final image. This procedure also corrects for dark current and zero-point offset ("fat zero"). Subsequently, we divided the images by a normalized flat-field frame to remove nonuniformities in the efficiency of the individual detectors. We found that the best flat field for these measurements was the result of an extensive series of images taken of overcast night sky at both 220 and 240 s duration. The difference of these exposures yields a flat field that is appropriate to that part of the detector gain curve for our integrations on NGC 1068. In practice, we observed the sky in the repeating sequence 240-220-220-240 s. By subtracting the difference of the second pair from the difference of the first pair, linear drifts in sky brightness are removed.

The final set of 22 K-band exposures were then assembled into a mosaic of the total image. For each individual frame, coordinates were determined from the known telescope offsets corrected for telescope drift via the SAO star observations. Approximately 25% of the pixels from each frame were removed based on our flat-field images: any pixel that did not flatten to within 1.5 σ of the mean were discarded. Zero-point differences between overlapping frames were attributed to errors in sky subtraction, and a constant was added to each frame to remove noticeable edge effects. In all cases, this constant amounted to no more than 10% of the image flux at this position. Individual frames were then placed in the mosaic, with averages taken in the regions of overlap. The final K image spans approximately 2'.5 (13.1 kpc) in each cardinal direction. A similar procedure was used to create the H map, which, however, is of poorer quality due to a lower quality flat field.

Our data are presented in a variety of ways in several figures. Due to the complexity of the central regions of NGC 1068, we present a schematic drawing in Figure 1. Contour maps of the brightness distribution in the two bands are shown in Figure 2, where the captions describe the noise levels in our final maps. A number of the features that we discuss are best seen in the series of surface plots presented in Figure 3. A series of

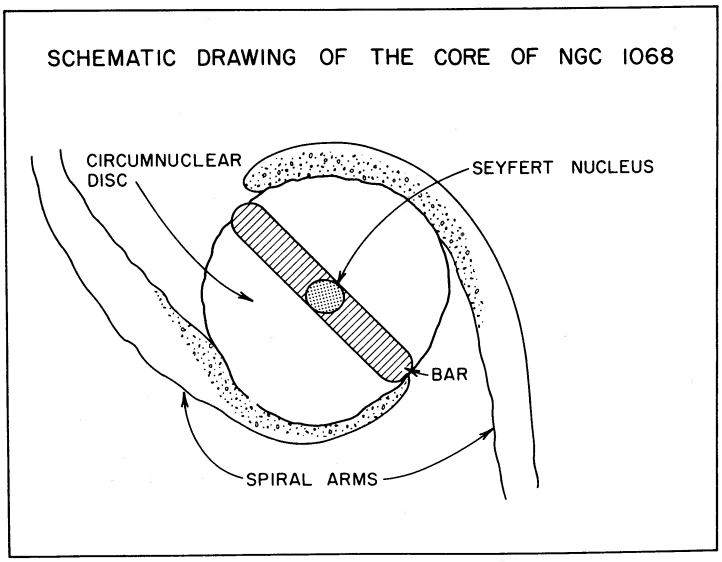

FIG. 1.—A schematic drawing of the central regions of NGC 1068 at near-infrared wavelengths. A variety of structures discussed in the text are labeled, which are probably most easily seen in our $V-K$ image (Fig. 5a [Pl. 9]).

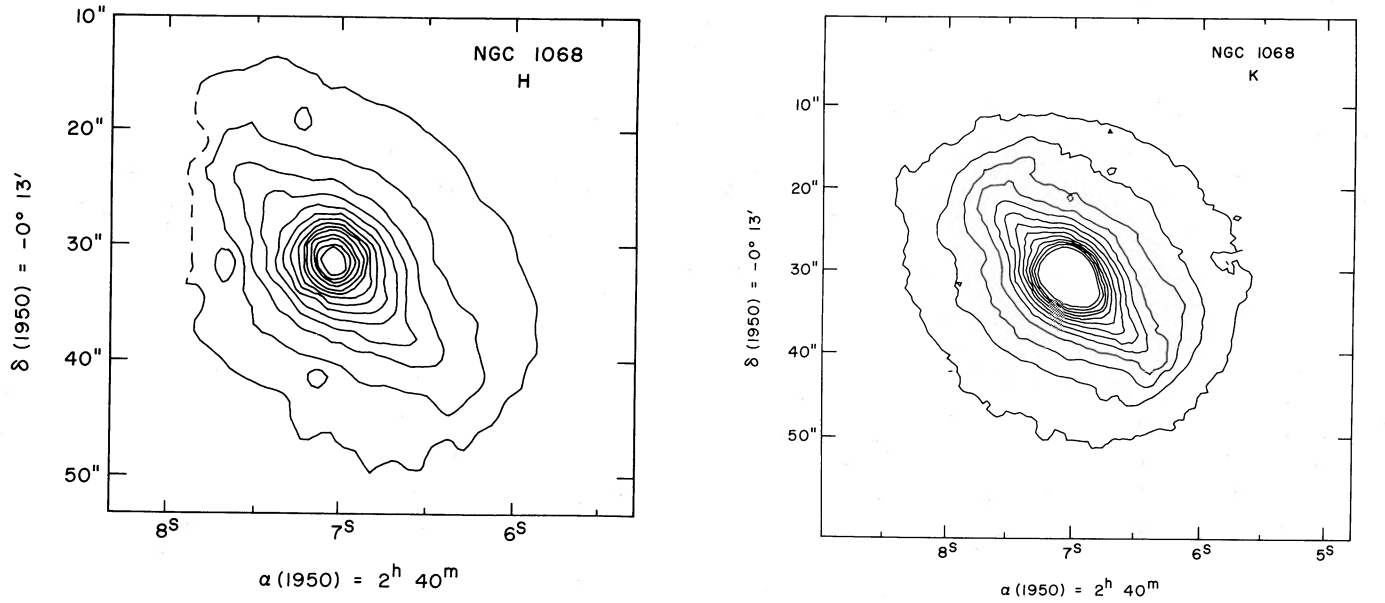

FIG. 2.—(*a*) The contour map of the *H* (1.6 μm) emission from NGC 1068. The lowest contour and each contour interval is 5.8×10^{-4} Jy arcsec^{-2} (m_H = 15.68 mag arcsec^{-2}). We estimate that the 1 σ noise level in this image is about 3×10^{-5} Jy arcsec^{-2} (m_H = 18.9 mag arcsec^{-2}). The extreme left side of the image was artificially set to zero to suppress the effects of rows of bad pixels in this region. The outermost contour is dashed to represent an uncertain distribution. (*b*) The contour map of the *K* (2.2 μm) emission from NGC 1068. The lowest contour level and each contour interval are equal to 2.9×10^{-4} Jy arcsec^{-2} (m_K = 15.87 mag arcsec^{-2}). We estimate that the 1 σ noise level is 1.5×10^{-5} Jy arcsec^{-2} (m_K = 19.1 mag arcsec^{-2}). Note that because our system was saturated by the bright nucleus, the maxima in both maps are truncated.

continuous-tone images are shown in Figures 4*a–e* [Plates 4–8]. Table 1 summarizes observational data on the galaxy.

III. DISCUSSION AND ANALYSIS

a) General Description of the Data and Nomenclature

We identify five clear structures in our data, which will be discussed in turn below where we also note past studies of these features. Readers are encouraged to refer to our schematic drawing (Fig. 1) for nomenclature. The small Seyfert 2 nucleus is by far the brightest feature in our images (Figs. 2, 3*a*, and 4*a*) but is surrounded by a bright and distinct bar (Figs. 3*b* and 4*b* probably show this feature best). The bar, in turn, is embedded within a disk or plateau of bright emission (Figs. 2, 3*c*, and 4*c*), from which faint, but distinct spiral arms emerge (Figs. 3*d* and 4*d*). We shall also refer to the star-forming ring region that surrounds the disk and is approximately coextensive with the inner segments of the spiral arms. The ring can also be identified with the region of maximum mid-infared and CO line emission and is the visually bluest part of the inner few arcmin of NGC 1068. Because of the likely role of the bar in confining the star-forming material, we discuss this ring largely in our subsection on the bar. We refer to this entire assembly, the inner ~1′ diameter region of NGC 1068, as the *core* of the galaxy. Note that the total extent of this giant galaxy is many times larger than the core region.

TABLE 1

PARAMETERS OF THE CIRCUMNUCLEAR REGION OF NGC 1068

Nucleus [α(1950; δ(1950)]	$2^h40^m07^s1$; −0°13′32″
Classification[a]	Sb(rs)II
L_B[b]	$1.7 \times 10^{10}\ L_\odot$
Far-infrared luminosity of the central ~1′[c]	$1.5 \times 10^{11}\ L_\odot$
Molecular gas mass[d]	$4.5\text{–}9 \times 10^9\ M_\odot$
Star-formation rate[e]	$100\ M_\odot\ \mathrm{yr}^{-1}$
Depletion time for the star-forming gas[f]	$\leq 7 \times 10^7$ yr
Mass of the stellar bar and disk[g]	$2\text{–}3 \times 10^{10}\ M_\odot$
Instantaneous star formation efficiency[h]	0.03

NOTE.—Adopted distance of NGC 1068 = 18.1 Mpc.

[a] Sandage and Tammann 1981.

[b] The total luminosity of the galaxy within the *B* passband, assuming $M_B = -22.26$ and $M_{B,\odot} = 5.48$.

[c] Telesco *et al.* 1984; Lester *et al.* 1987; excludes Seyfert nucleus.

[d] Scoville, Young, and Lucy 1983; Myers and Scoville 1987; Thronson *et al.* 1987; Kaneko *et al.* 1988.

[e] Estimated from the far-infrared luminosity and a Salpeter initial mass function from 0.1 → 100 $M_\odot$ (Thronson and Telesco 1986).

[f] The molecular mass divided by the star-formation rate; probably an upper limit due to the assumption of perfect efficiency in long-term star formation.

[g] Values calculated from the near-infrared photometry and the observed rotation curve. See the discussion of § III*b*.

[h] The current mass of young stars, derived by assuming a Salpeter function from 0.1 → 100 $M_\odot$, divided by the mass of star-forming gas.

i) *The Seyfert 2 Nucleus*

The bright nucleus of NGC 1068 has been studied in detail for more than 80 years, even before "spiral nebulae" were universally known to be extragalactic. In this Ph.D. thesis, a study of the composition of these nebulae, Fath (1909) presented a visual spectrum of the nucleus, identified a number of emission lines, and argued that the center of this object is comprised of very distant stars, surrounded by or mixed with excited gas. Not surprisingly, Slipher (1917) also studied this galaxy in detail and found its emission lines to be very broad (see also Campbell and Moore 1918). Decades later, Seyfert (1943) included NGC 1068 in his original list of six spiral galaxies with unusually broad, high-excitation nuclear emission lines. He concluded that the bright nuclei of these galaxies were not similar to giant H II regions. Beginning in the mid-1950s, the number of studies of the emission from luminous extragalactic nuclei increased dramatically (see the review of this

PLATE 4

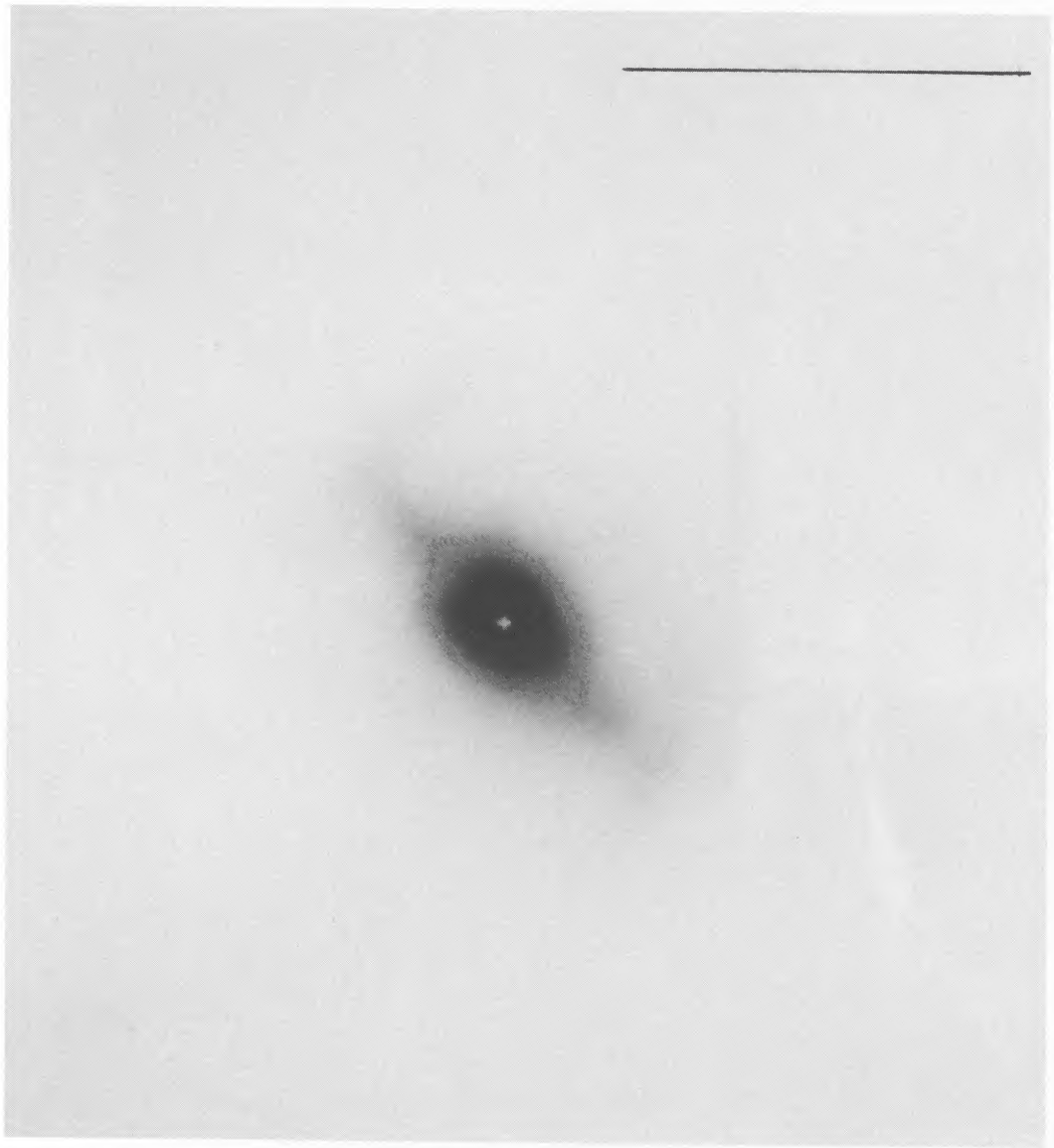

FIG. 4*a*

FIG. 4.—(*a–d*) A series of four continuous-tone images of the *K* emission from the center of NGC 1068, each with a different maximum cutoff. From the first through the last image, they have the same cutoffs as do the surface plots in Fig. 3. A small white cross appears at the position of the nucleus and a 30″ long east-west bar is drawn in each figure. North is up, east is to the left. (*e*) A continuous-tone image of the *H* emission, scaled to show about as much low-level detail as Fig. 4*b*. The brighter emission looks very similar to that at *K*. A small white cross appears at the position of the nucleus and a 30″ long east-west bar is drawn in the figure. North is up, east is to the left.

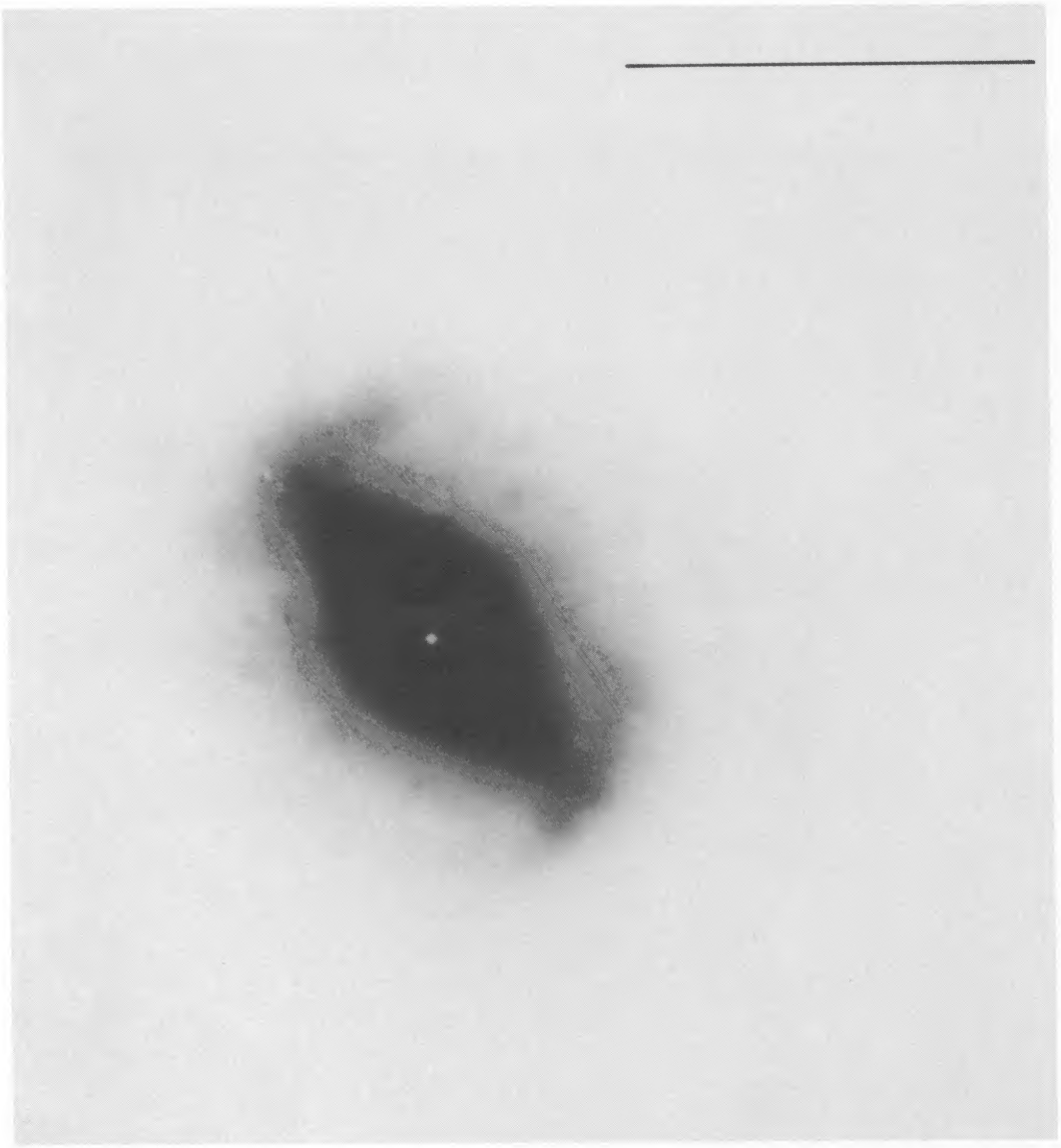

FIG. 4*b*

PLATE 6

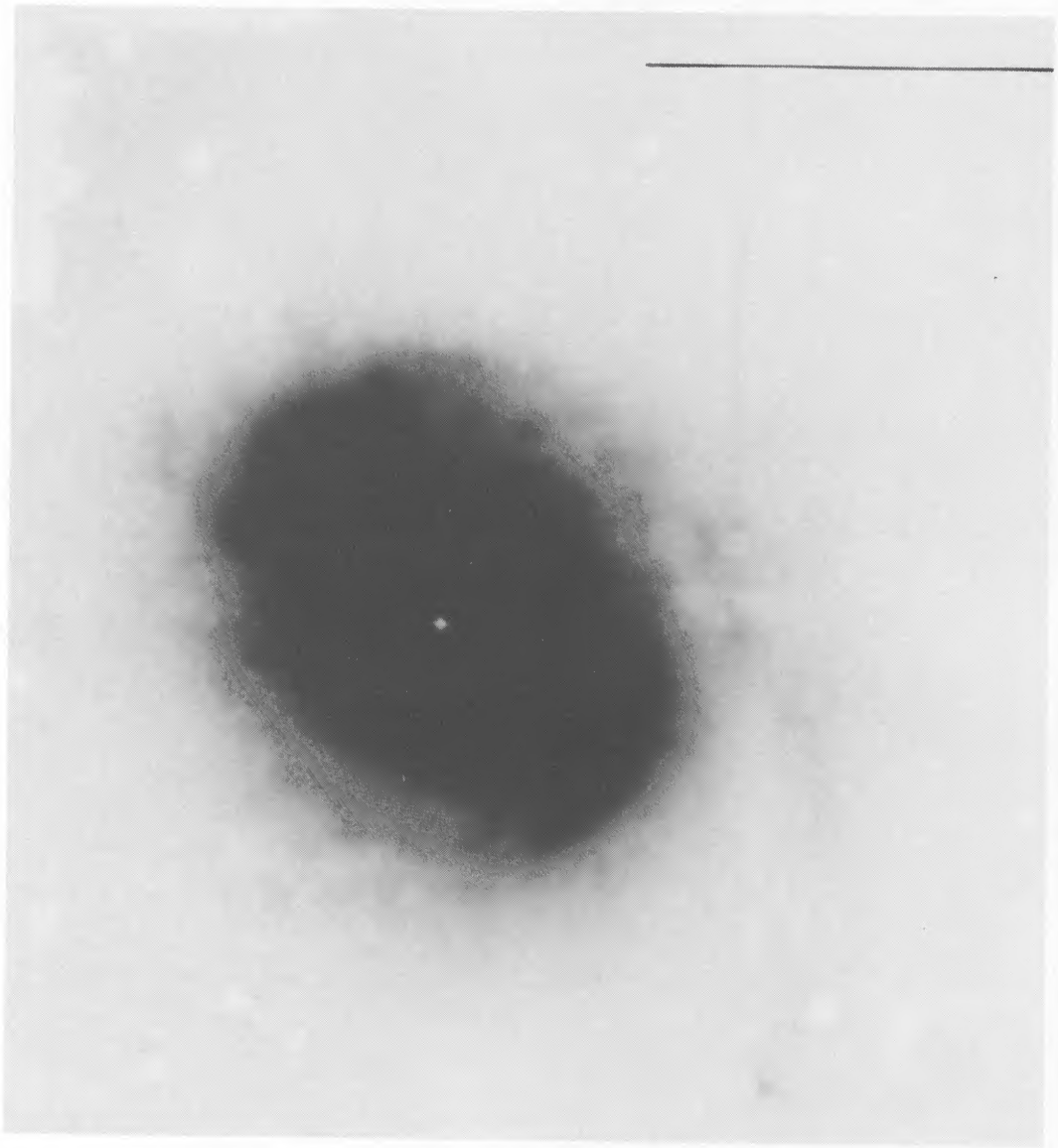

FIG. 4*c*

THRONSON *et al.* (*see* **343**, 160)

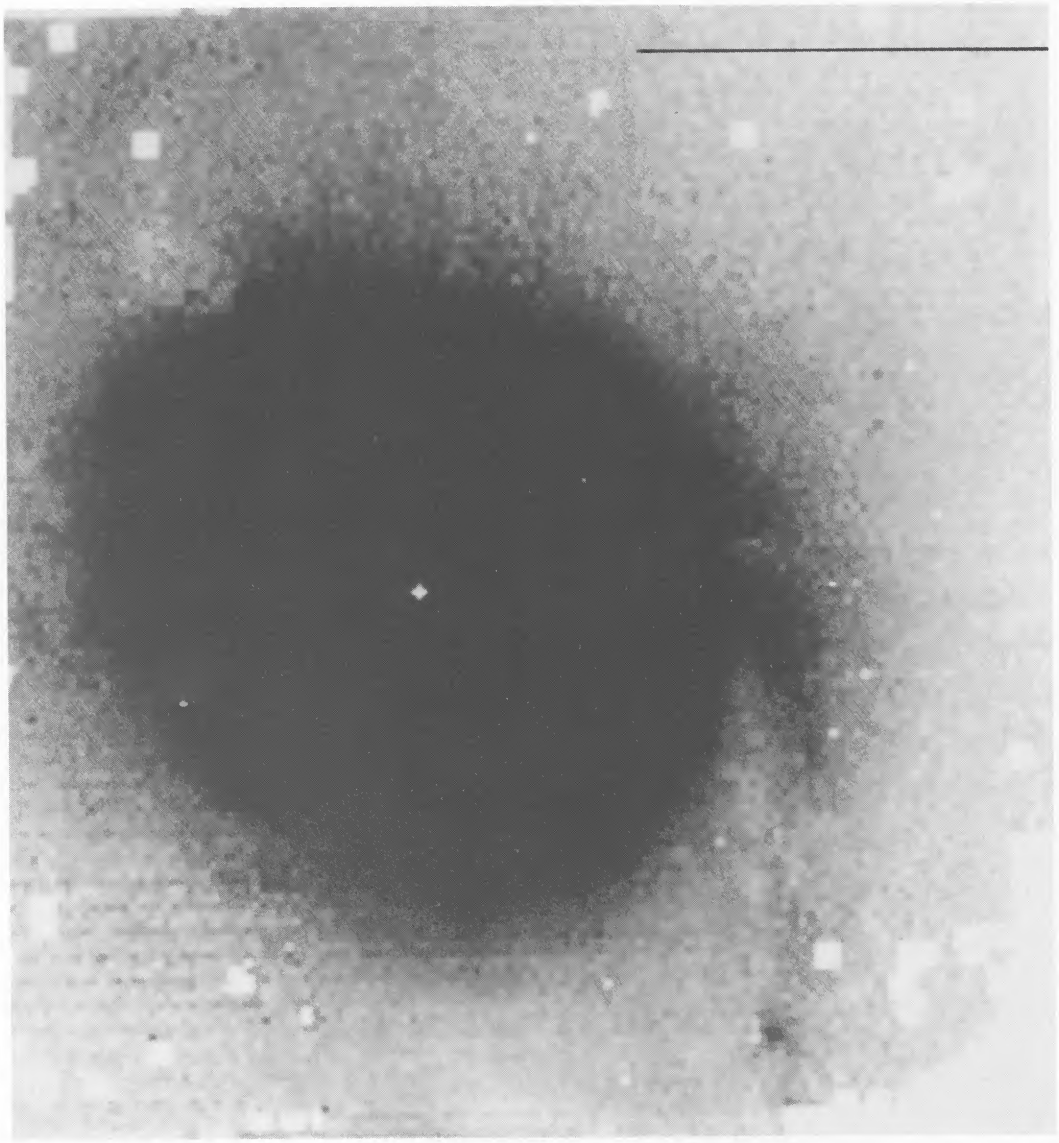

FIG. 4*d*

THRONSON *et al.* (*see* **343**, 160)

PLATE 8

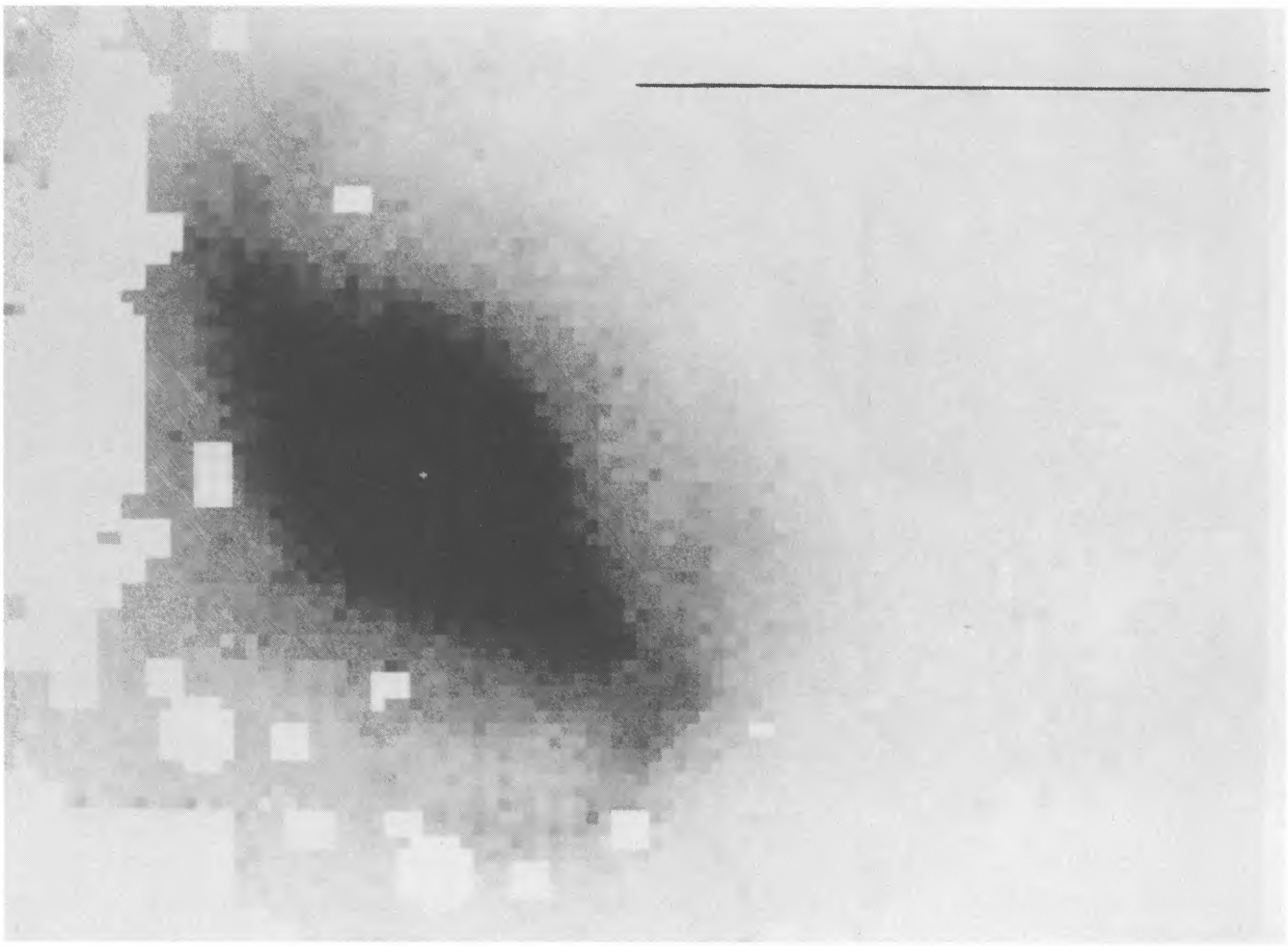

FIG. 4*e*

THRONSON *et al.* (*see* **343**, 160)

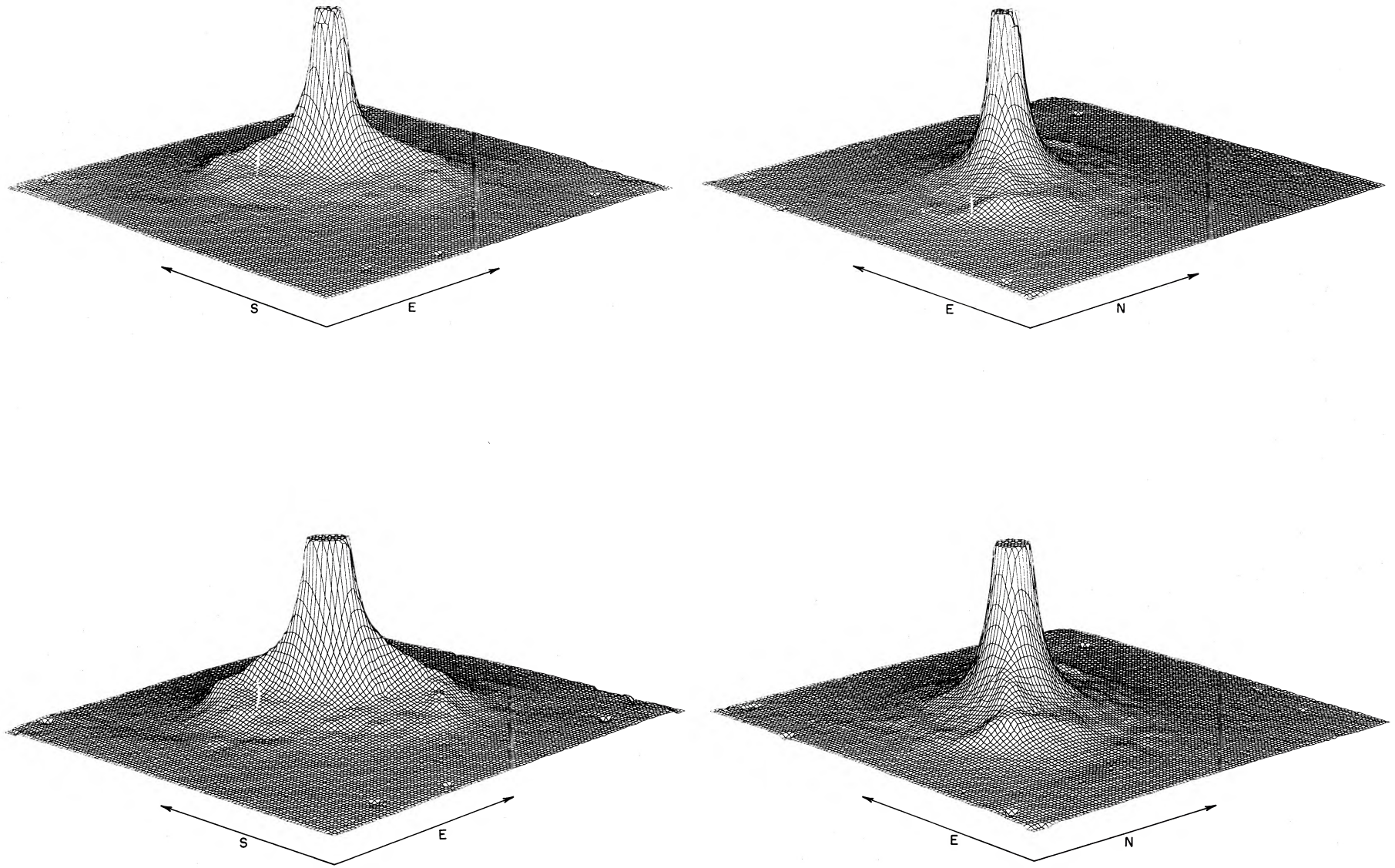

FIG. 3.—A series of eight surface plots of the K emission from NGC 1068: two orientations of each of four different maximum values. Each element of the surface is one pixel (0.″59) on a side and the veritcal scale is linear. The left figure of each pair recreates the flux distribution as it appears from the northwest (*upper right*) corner of Figs. 2 and 4, while the right figure shows the flux distribution as it would appear from the southwest (*lower right*) corner of Fig. 2. The maximum cutoffs are, from the first through the last, 8.62×10^{-3} Jy arcsec^{-2} ($m_K = 12.19$ mag arcsec^{-2}), 5.75×10^{-3} Jy arcsec^{-2} ($m_K = 12.63$ mag arcsec^{-2}), 2.87×10^{-3} Jy arcsec^{-2} ($m_K = 13.38$ mag arcsec^{-2}), and 1.44×10^{-3} Jy arcsec^{-2} ($m_K = 14.13$ mag arcsec^{-2}).

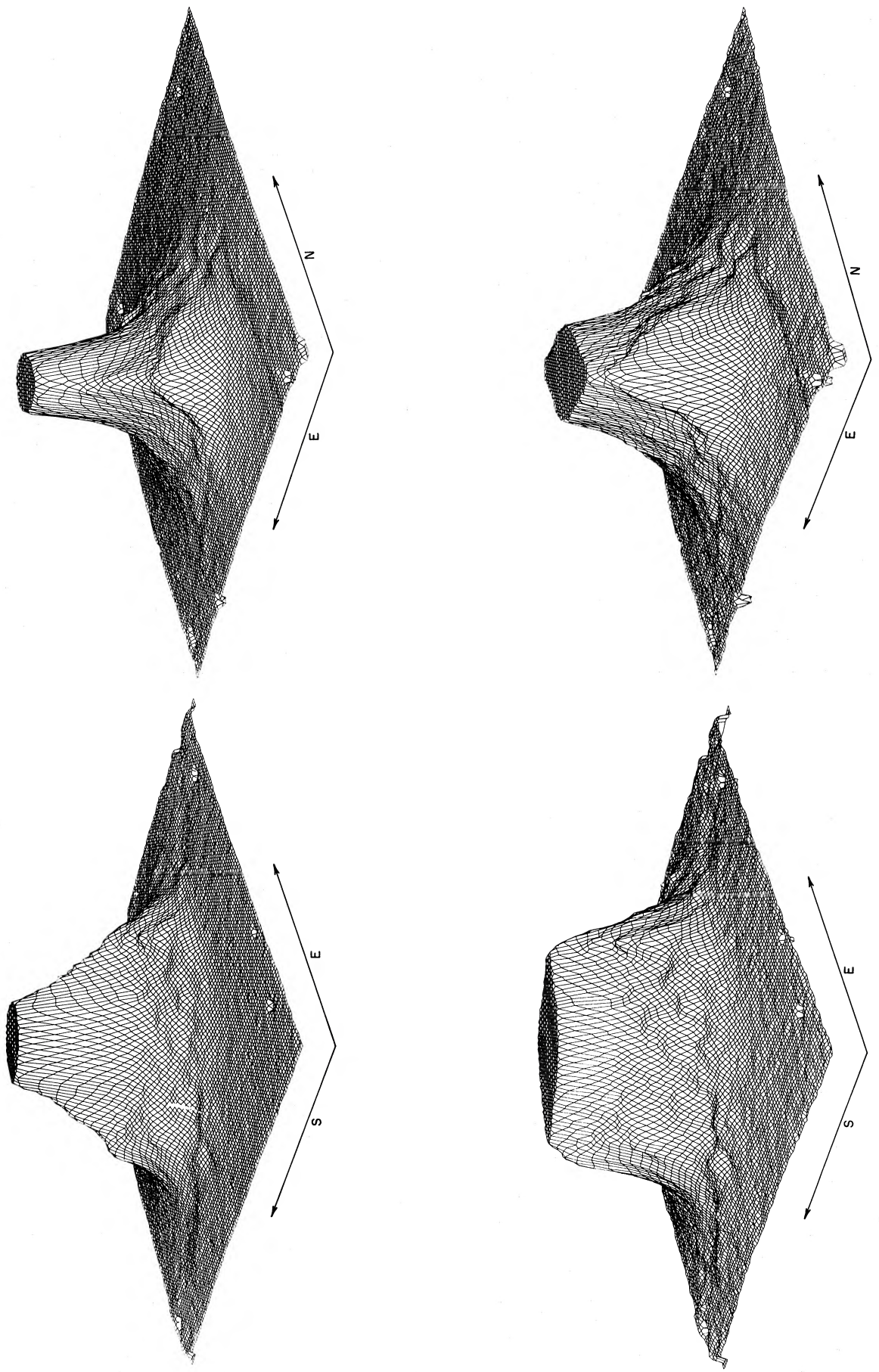

FIG. 3.—*Continued*

early work by Burbidge 1970). Detailed observations by Code (1959), Osterbrock and Parker (1965), Visvanthian and Oke (1968) stand out from this period as they emphasized the unusual nature of the nucleus of NGC 1068 and led to early descriptions of the mechanism(s) of excitation.

The small-scale structure of the visual and near-infrared emission from the pointlike Seyfert nucleus has been considered in detail by Hall *et al.* (1981) and McCarthy *et al.* (1982). The latter authors used infrared speckle interferometry to find that the 2.26 μm emission is dominated by a bright center, less than 0".2 (20 pc) in diameter. They also found that there is significant near-infrared emission surrounding this bright maximum, but they were not able to describe its structure in detail. Hall *et al.* proposed a model for the nucleus of the galaxy in which about 25% of the near-infared light arises from a late-type stellar population, while hot dust, presumably heated by the central Seyfert engine, contributes the majority of the emission in the near-infrared. This description, then, generally supports the original model for the nucleus by Fath (1909).

Because our primary goal was to study the fainter emission surrounding the nucleus, our integration times were so long that the emission from the nucleus saturated our system. For this reason, our images should be considered only approximations for this component and the reader is referred to McCarthy *et al.* or Scoville *et al.* (1988) for more accurate representations of the nucleus itself. Our contour maps and images at radii greater than about 3" from the nucleus are reliable. Close to the nucleus we find modest deviations from a simple point source that might be related to nuclear activity in this object. For example, after careful comparison with stellar images obtained with our camera, the southwest side of the nucleus appears to have a shoulder or bulge, in excess of the luminous bar (next section), which is not easily represented in the figures that we present here. A number of other observers have more successfully found somewhat similar "bulges" close about the nucleus (e.g., at mid-infrared wavelengths by Tresch-Fienberg *et al.* 1987; at radio wavelengths by Wilson and Ulvestad 1982, 1987). A gray-scale $B-R$ image (Fig. 4 in Schild, Tresch-Fienberg, and Huchra 1985) indicates that the southwestern side of the bright nucleus is extremely red, leading one to expect excess near-infrared emission from the same region. The apparent *visual* redness of this part of the inner core of the galaxy suggests enhanced dust obscuration surrounding a stellar condensation. Perhaps this emission corresponds to a thick disk or torus which has been proposed as a possible confinement mechanism for the radio jets and the highly ionized visual emission features that seem to emanate from the center of the galaxy (see, e.g., Antonucci and Miller 1985; Baldwin, Wilson, and Whittle 1987; Pogge 1988). Asymmetry to the southwest would then complement the asymmetry to the northeast in the [O III]/(Hα + H II) map (Fig. 2 in Pogge), which is what one would expect if the axis of the torus were tilted with respect to the plane of the disk.

ii) *The Bar and Its Relation to Active Star Formation*

The most striking aspect of our near-infrared images is the bar, running from the northeast to southwest at a position angle of 45° ± 0°.5. Our Figures 2, 3*b*, *c*, and 4*a*, *b*, *d* show this feature clearly. It is a well-defined structure, about 34" ± 1" (3.0 kpc) in extent, depending slightly on the surface-brightness contour at which this is measured. A barlike structure has occasionally been referred to in the literature or inferred as part of an analysis (e.g., Alloin *et al.* 1981; Baldwin, Wilson, and Whittle 1987), but this dominant structure of the central ~2 kpc of NGC 1068 was not truly revealed until infrared imaging discovered it (Scoville *et al.* 1988; G. Bothun 1988, private communication). For example, the detailed very red (0.8 μm) image of this region of the galaxy by Ichikawa *et al.* (1987) shows only an oval-shaped elongation and no evidence of a sharp bar. This situation is a repetition of one study of the large face-on spiral NGC 1566, which was not known to possess a central bar until near-infrared mapping demonstrated otherwise (Hackwell and Schweizer 1983). These latter authors suggested that very many grand design spirals may have a stellar bar not easily detectable at visual wavelengths, perhaps as a consequence of a very different stellar population in the bars compared to that of the surrounding region.

The spatial proximity of the bar to regions of extremely luminous mid- and far-infrared emission in NGC 1068 (Telesco and Decher 1988) makes it likely that the bar is directly responsible for the extremely active star formation for which the core of NGC 1068 is so famous (e.g., Burbidge 1970; Telesco *et al.* 1984; Weedman and Huenemoerder 1985; Lester *et al.* 1987; Telesco and Decher 1988). Furthermore, the local maxima in the millimeter-wave CO emission (Myers and Scoville 1987; Kaneko *et al.* 1988) lie near the ends of the bar, while the central disk of the galaxy appears swept nearly clean of large amounts of molecular material. It is reasonable to conclude that the bar plays the major role in confining or organizing the star-forming material into the structures that surround the central region of NGC 1068. With the molecular material localized to truncated spiral arms or to a partial ring surrounding the disk, star-forming activity must at present also take place primarily in the region surrounding the disk and outside the bar. In support of this view, Telesco and Decher (1988) find the 10 μm flux from hot dust to be distributed throughout the region of maximum CO line emission, but not closely associated with the bar itself. Telesco and Decher go on to argue that the gravitational potential of the bar has assembled the pair of truncated spiral arms as the orbits of circumnuclear interstellar gas change over 90° in azimuth between a pair of inner Lindblad resonances. Additional support for active star formation distributed roughly circularly outside the circumnuclear disk may be seen in the beautiful color image of the central ~40" of the galaxy by Véron-Cetty and Véron (1983). They show a pale orange central core, surrounded by a ring of rich blue emission (see also Lausten, Madsen, and West 1987; Ichikawa *et al.* 1987). This ring is also evident in the *U* image by Stockton (displayed in Telesco *et al.* 1984), the color profiles of Schild, Tresch-Fienberg, and Huchra (1985), and in Hα images (Balick and Heckman 1985; Atherton, Reay, and Taylor 1985; Pogge 1988; Young, Kleinmann, and Allen 1988). Schild, Tresch-Fienberg, and Huchra find that while the average visual colors of the central ~1'.5 diameter disk of NGC 1068 are similar to those of the old galactic cluster M67, there are regions of blue enhancements associated with the surrounding spiral arms. The blue ring of presumably stellar light is approximately spatially associated with the CO maxima (Myers and Scoville 1987; Kaneko *et al.* 1988) and the region that dominates the mid-infrared emission from hot dust (Telesco and Decher 1988). In a conventional picture of the flow of gas through a bar (e.g., Roberts, Huntley, and van Albada 1979; Huntley 1980; Schwarz 1981), gas swept up by the outer part of the bar can be carried to its ends, which becomes a likely site of active star formation, while gas col-

lected in the inner bar is funneled to the nucleus, which presumably could fuel the powerful Seyfert engine in NGC 1068.

Multiaperture photometry and extensive mapping now exists from the ultraviolet through the near-infrared for the inner 3 kpc of NGC 1068, which we shall use to investigate the composition of the bar, disk, and ring. In addition, a modest number of other galaxies have been observed at the wavelengths most sensitive to the stellar populations, ultraviolet through near-infrared. We shall compare the colors of NGC 1068 with, in particular, those of the well-known starburst galaxy NGC 3310 (Telesco and Gatley 1984), and the two late-type face-on spirals, NGC 1566 (Hackwell and Schweizer 1983) and IC 342 (Thronson, Hereld, and Sloan 1989). One of the major justifications for near-infrared observations of galaxies is its relative insensitivity to rare, hot stars, thus allowing the underlying distribution of more abundant stellar populations to be revealed. Stars dominate the near-infrared emission throughout this wavelength range: as we shall show below, the visual and near-infrared colors of the bar and disk of NGC 1068 are consistent with a stellar population, with modest contributions from the effects of dust. However, although near-infrared photometry of galaxies has been available for a couple decades, reliable determination of the stellar mass distribution remains a *Leucadia*[4] of modern astronomy: a unique stellar composition cannot be derived from broad-band photometric data alone.

Central to our analysis of the core of NGC 1068 is a pair of color-difference images. R. Schild very kindly made available to us a visual CCD image of the galaxy used in his earlier work (Schild, Tresch-Fienberg, and Huchra 1985). Figure 5*a* [Pl. 9] is a $V-K$ image of the central $\sim 1'$ of the galaxy. Our near-infrared image was saturated at the position of the nucleus, and the visual data suffer a "bloom trail" slightly west of the nucleus, both of which make the center of the image useless for analysis. However, several of the important structures of the core of the galaxy appear clearly as redder features (lighter shades of gray in the figure). The near-infrared bar appears sharp and distinct, embedded within a darker (bluer) surrounding disk. This image graphically demonstrates that near-infrared observations were necessary to reveal that NGC 1068 is a strongly barred galaxy. The star-forming ring is clear, forming a nearly unbroken reddish circle around the bar/disk region. Finally, emanating from the ring is one clear red arm that can easily be traced through almost 180° and another opposite, but less distinct arm. The spiral arms will be discussed further in § III*a*(iv).

In Figure 5*b* (Pl. [10]) we present an $H-K$ image of the core, where in this case redder regions appear darker, the opposite of Figure 5*a*. This image is of poor quality, due to our more limited data at H. Again, our data at the position of the nucleus are unreliable. Nevertheless, the red star-forming ring is easily distinguished, as is part of a red spiral arm just to the west of the ring. However, the central bar is barely visible, merged into the similar $H-K$ color of the surrounding disk, in sharp contrast to the $V-K$ image. We begin our discussion of the composition of the core components of NGC 1068 by suggesting that, based on the $V-K$ and $H-K$ images, a major fraction of the K emission in the ring and arms must arise from some component that is (1) strongly confined to both structures, since our color-difference images trace them so well, and (2) different from the component that reveals the bar in the $V-K$ image, since this structure has almost disappeared in our $H-K$ image.

We can rule out emission from photospheres of newly formed stars as making a major contribution to the flux at K from the bar or its surrounding disk (this does not include the star-forming ring, obviously). In the first place, there is little or no mid-infrared flux from hot dust or CO line emission from star-forming gas that is unambiguously associated with either of these components (Myers and Scoville 1987; Telesco and Decher 1988; Kaneko *et al.* 1988). Furthermore, the visual color of the bar/disk region is similar to that of an older open cluster in the Milky Way (Schild, Tresch-Fienberg, and Huchra 1985; Véron-Cetty and Véron 1983) and the bright blue visual emission, presumably from newly formed stars, *surrounds* the disk in the partial ring structure. In the data that are available to us, primarily the multiwavelength images, the star-forming ring appears to be made up of a population that is very different from that of either the bar or disk.

To quantify our conclusions, we use the variety of observational and theoretical color-color diagrams that have been produced in recent years. Here we emphasize the work by Struck-Marcell and Tinsley (1978), Aaronson (1978), and Telesco and Gatley (1984), all of whom produced useful two-color diagrams for a variety of wavelengths and for many objects that might have a composition similar to NGC 1068. In addition to our own H and K images, we use the near-infrared multiaperture photometry of Scoville *et al.* (1988) and the summary of visual data in Schild, Tresch-Fienberg, and Huchra (1985). We begin with a discussion of visual and near-infrared colors for two annuli presented in Table 2. Subtraction of the emission from a 5″ diameter circular aperture removes the contribution from the extremely bright Seyfert nucleus. The smallest annulus is dominated by light from the bar/disk region (refer to our schematic diagram in Fig. 2), and the second largest should be dominated by emission from the bright star-forming ring (see also Véron-Cetty and Véron [1983] as well as Ichikawa *et al.* 1987). We have included an extremely large annulus—the largest for which we could find reliable data—as an estimate of the colors for the entire galaxy. The estimated uncertainty in the multiannular colors are 0.05 mag for the visual data and 0.1 mag for the near-infrared

TABLE 2

SOURCE COLORS IN SELECTED ANNULI

	ANNULUS OR APERTURE:			
COLOR	5″ (dia.)	5″–30″[*a*]	30″–55″[b]	4.′7 (dia.)[c]
V	11.90	10.60	11.15	8.9
$B-V$	0.85	0.85	0.70	0.70
$U-B$	−0.10	0.10	0.05	0.05
$V-K$	4.6	3.3	3.6	...
$J-H$	1.1	0.7	0.7	...
$H-K$	1.4	0.2	0.3	...

NOTES.—[*a*] bar and disk, [*b*] star-forming ring and neighboring spiral arms, and [*c*] largest aperture in available data set.

Photometry taken from the compilations of Schild, Tresch-Fienberg, and Huchra (1985); Scoville *et al.* (1988); and this work. $V-R = 0.75$ throughout the region sampled. Uncertainties in the colors are estimated to be ± 0.05 at visual and ± 0.1 magnitudes in the near-infrared due to the smaller number of observations available at these longer wavelengths. No corrections for extinction have been applied.

[4] The promontory from which desponding Sappho threw herself when she discovered that her love for Phaon was in vain. Thus, a *Leucadia* is a site of obsession and frustration.

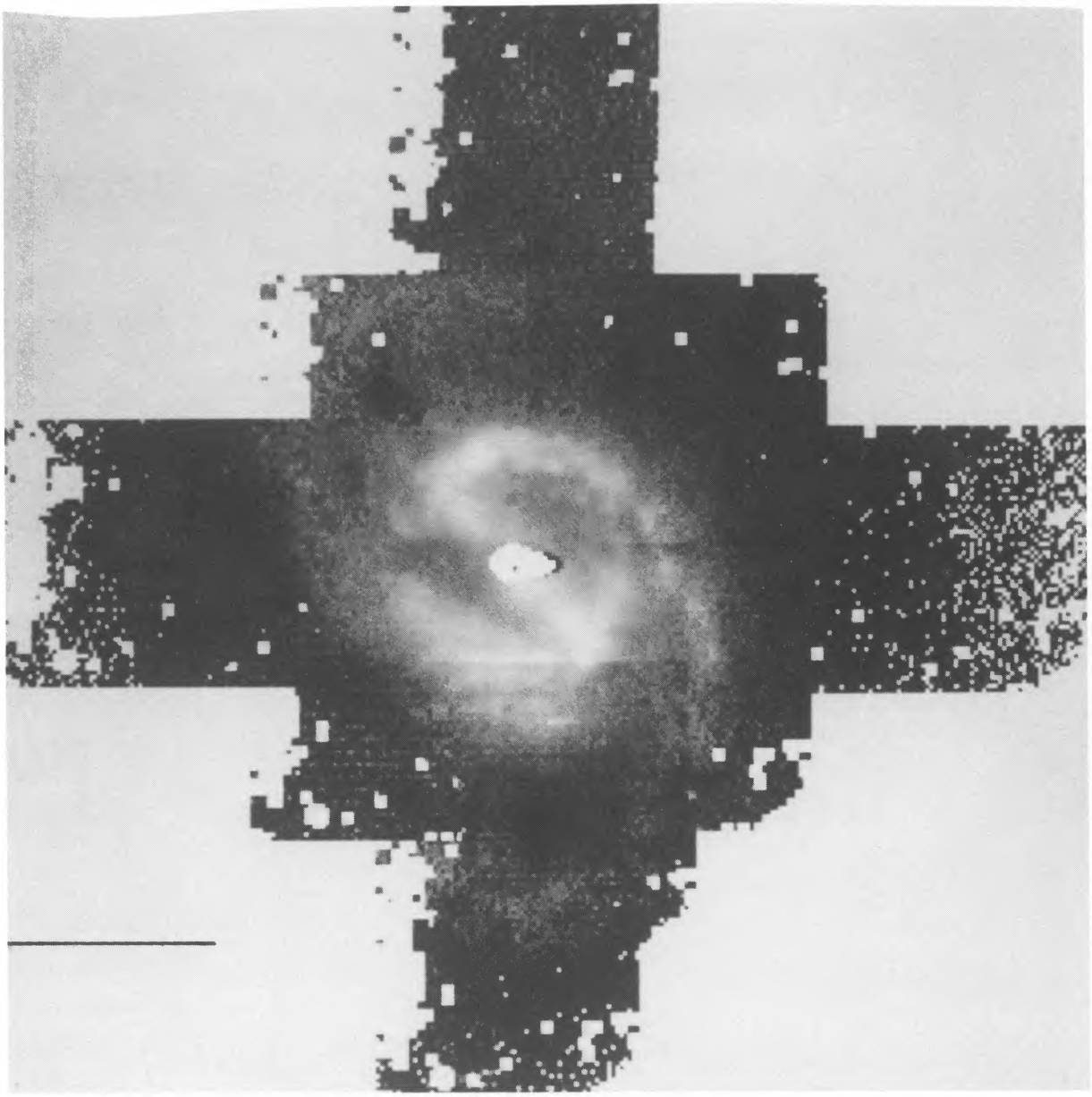

FIG. 5*a*

FIG. 5.—(*a*) A $V-K$ image of NGC 1068, which demonstrates that the central bar is exclusively an infrared feature. The redder emission appears as a lighter shade of gray, and the white region in the center is the location of unreliable near-infrared or visual data. A number of bad pixels are scattered throughout the image. A small black cross is at the position of the nucleus and a 30″-long east-west bar is shown. R. Schild kindly supplied the V CCD data. North is up and east is to the left. (*b*) An $H-K$ image of NGC 1068, where redder emission appears as darker gray. The black region in the center is the location of unreliable H or K data. A small white cross is at the position of the nucleus and a 30″ long east-west bar is shown. This image is of poor quality due to the poorer flat field used for the H data.

THRONSON *et al.* (*see* **343**, 164)

PLATE 10

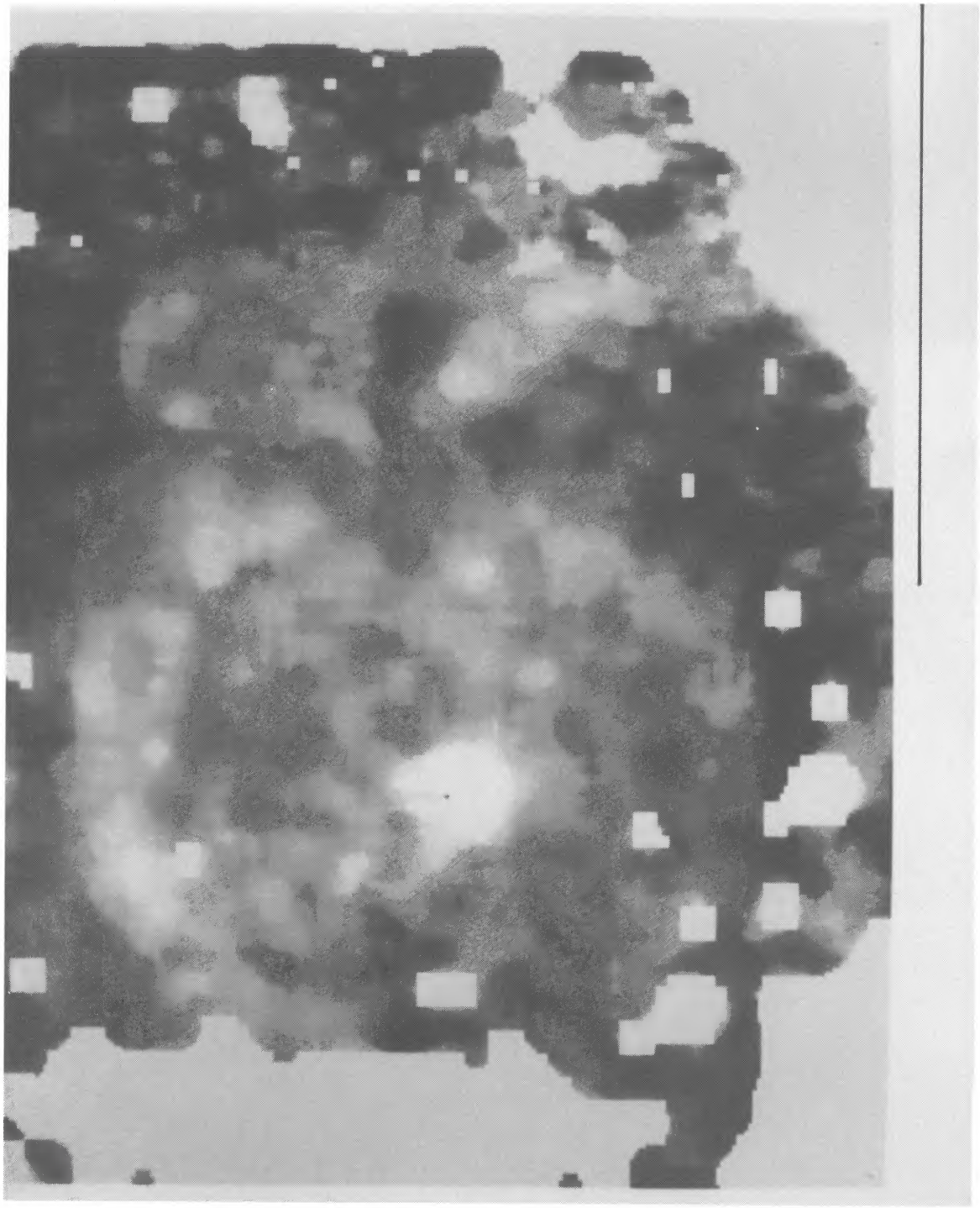

FIG. 5b

THRONSON *et al.* (*see* **343**, 164)

observations. These uncertainties are larger than usually quoted in the literature due to significant brightness and color variations as a function of position in the core of this galaxy (see the diagrams of color variations as a function of radius presented by Schild, Tresch-Fienberg, and Huchra [1985]; refer also to Ichikawa *et al.* [1987] and to our Fig. 5). In addition, although there is a great deal of photometry of NGC 1068, not all wavelengths have been observed with all apertures and some interpolation was necessary in extracting brightnesses from data in the literature. The uncertainty is about the size of the variation in some of the colors among the annuli in our table.

Telesco and Gatley (1984) show the distribution of the giant-dominated nuclei of normal spiral and elliptical galaxies in the near-infrared ($J-H$, $H-K$) two-color diagram, along with vectors that show changes in the colors as different additional components (e.g., hot dust, obscuration, young stars) are included. The near-infrared colors of both annuli in Table 2 are similar to those of giant-dominated nuclei of normal galaxies—that is, $J-H = 0.75 \pm 0.05$, $H-K = 0.25 \pm 0.05$—except for about an 0.1–0.2 mag "excess" in the brightness at K in the core of NGC 1068. Following the figure in Telesco and Gatley, excess K emission can be explained by a modest (10%–20%) enhancement of the 2.2 μm flux from hot dust above that expected from an older stellar population. Scoville *et al.* (1988) also concluded that there is a small amount of dust emission at K in the core. We note that warm dust emission is not at all surprising in an object such as NGC 1068 with an intense stellar radiation field, perhaps as a result of low-level star formation in the bar and disk. However, the $J-H$ colors, which are sensitive to hotter stellar photospheres and overlying dust obscuration, show no evidence for a major contribution from either component to a cool giant population in NGC 1068 for either of the annuli in our table: the $J-H$ color is indistinguishable from that of the older stellar populations in ellipticals and the bulges of spirals.

We contrast the bar/disk colors of NGC 1068 with the results of the photometry of the starburst galaxy NGC 3310 (Telesco and Gatley 1984). This galaxy's colors in its inner region are bluer in $H-K$ and, perhaps, $J-H$, which indicates a larger fraction of young stars and a relatively smaller contribution from hot dust. Similarly, the near-infrared bar/disk colors of the barred spiral NGC 1566 (Hackwell and Schweizer 1983) and the colors of the central disk in the dusty spiral IC 342 (Thronson, Hereld, and Sloan 1989) are close to those of NGC 1068, within the uncertainties. We conclude that the majority of near-infrared light from the central core of NGC 1068 arises from an older stellar population, with a 10%–20% contribution from hot dust.

Our conclusions are unchanged by also including visual data, which, because of their sensitivity to hotter stellar photospheres, allow us to investigate the contribution from younger stars. Aaronson (1978) graphed the $U-V$ and $V-K$ colors for all major galaxian morphological types. NGC 1068, classified as a Sb(rs)II, has colors appropriate for an intermediate spiral, modified by an excess K brightness of about 0.1–0.2 mag as we found above.

A small amount of visual extinction internal to NGC 1068 would affect the observed $V-K$ colors and our Figure 5*a* somewhat similarly to the effects of warm dust emission, but significant dust obscuration seems unlikely since the visual images and photometry of the bar/disk region show no obvious signs of large amounts of obscuring material. However, Young, Kleinmann, and Allen (1988) used visual line imaging to map the visual extinction in the core of NGC 1068. They estimated $A_V \approx 0$–5 mag over the bar and disk, which means that the visual colors in our table may have to be corrected by a large factor to account for this extinction. Quantifying this correction using the results of Young, Kleinmann, and Allen (1988) will be difficult for at least three reasons. First, out of necessity, Young, Kleinmann, and Allen used a model for the wavelength-dependence of the extinction that is based on grains in the Milky Way. Second, they adopted a formulation to derive the extinction from the line data that assumes the dust overlies the emission sources, rather than is mixed in, which we feel is more realistic. Third, there can be systematic effects in using a broad-band filter to derive the continuum emission from galaxies. Nevertheless, these authors derived a maximum dust extinction that lies roughly along the bar that is revealed by near-infrared mapping. It is therefore possible that the reason that the strong bar was missed by imaging at visual wavelengths was that it was obscured from view and longer wavelength observations were necessary to find it. Curiously, visual images of the core of NGC 1068 do not obviously show the bands of obscuration that other dusty barred galaxies show (Ichikawa *et al.* 1987).

iii) *The Disk*

Complicating study of the center of the galaxy at visual wavelengths has been the extremely bright disk of emission, within which the bar and the nucleus appears embedded. Keel and Weedman (1978) identified this disk as the brightest yet studied (see also Ichikawa *et al.* 1987). Our Figures 3*c*, *d*, and 4*c*, *d* show this region clearly. It surrounds the distinct bar and, because of the large area that it covers, contributes a significant fraction of the near-infrared light from the central arcminute of the galaxy.

One conventional view of galactic bar formation has individual stars moving in loops around the nucleus, with alignment of the elongations of the loops to produce the bar instability. Stars orbit the galaxian nucleus, moving into and out of the bar (see, e.g., Sellwood 1981). That is, a bar is a density-wave feature and the stars of which it is made are the same as those in the surrounding disk. Thus, in this view, the discussion in the preceding section on the population applies equally strongly to both the bar and the surrounding disk within which the bar is embedded. However, dust obscuration derived by Young, Kleinmann, and Allen (1988) lies along the bar, preferentially hiding it at shorter wavelengths. Therefore, images in $V-K$ reveal the bar as distinctly different from the disk, but the bar appears to be the same color as the disk in $H-K$ because the stellar population is similar and the dust has little effect at near-infrared wavelengths.

Hackwell and Schweizer (1983) proposed a different explanation for the observations of NGC 1566. This galaxy likewise has a significant infrared barlike structure obscured at shorter visual wavelengths, but Hackwell and Schweizer suggested that the bar might have a different stellar population than its surrounding disk with little mixing of the disk material with the bar material. Hackwell and Schweizer proposed that the near-infrared bar that they found in NGC 1566 was very red due to a significant contribution from carbon stars, which appear around a few times 10^9 yr after their main-sequence precursors are born. This is an attractive explanation for NGC 1068 as well, since our argument that there is little active star formation taking place within the bar/disk region at present

does not preclude active star formation in the recent past. Moreover, emission from carbon stars cannot easily be distinguished using near-infrared photometry from that of any other evolved star, which would explain why the bar appears to merge with the surrounding disk in our $H-K$ image. Thermal emission from dust, for example, does not have this effect, which is why the arms are easily seen in the $H-K$ image (following section). It is possible that young, red supergiants could also produce a near-infrared bar, but we have argued that there seems to be little observational support for extensive current star formation in the bar. Finally, we note that the bar/disk complex is in the region of rigid-body rotation (summarized by Telesco and Decher 1988) in the galaxy, and there may be little azimuthal mixing between components that make up the bar and those that make up the disk. Thus, if the bar and disk formed at different times, or with different rates of star formation, stellar population differences between the two structures might last a long time.

iv) *The Star-Forming Ring and Spiral Arms at Near-Infrared Wavelengths*

Although spiral arms are distinctly blue at visual wavelengths, they should have a significant population of older stars and, perhaps, warm dust, and would be easily traced in near-infrared images (e.g., Hackwell and Schweizer 1983; Elmegreen and Elmegreen 1985). NGC 1068 is no exception and our Figures 2*d*, 4*d*, and 5 show the spiral structure that surrounds the much brighter inner disk and bar region. Furthermore, a number of features in visual-wavelength images can be found in our images as well (cf. our Fig. 3; Fig. 1 in Véron-Cetty and Véron 1983; Fig. 4 in Schild, Tresch-Fienberg, and Huchra 1985; Ichikawa *et al.* 1987). For example, the northeast and southwest H II complexes found by Balick and Heckman (1985) are clearly visible in our images.

The spiral arms, apparently connecting to the ends of the central bar at the star-forming ring, stand out sharply as red features in $V-K$ and $H-K$ images (Figs. 5*a* and 5*b*). It is easy to trace the red spiral arms over almost 180° in our Figure. 5. (Note that the spiral arms are not necessarily red, but our color-difference images show that they are *redder* than the surrounding galaxian disk.) It is not immediately obvious whether the color is due to brighter emission at K (e.g., warm dust) or depressed emission at V (e.g., obscuration), but we argue that the most likely is the former, rather than the latter.

This conclusion is based in part on our discussion in § III*a*(ii), where we found that small amounts of warm dust emission is a ready explanation for the integrated K emission from the circumnuclear core region. More persuasive is the comparison between Figure 5*a* and 5*b*: the ring and arms are redder in both color-difference images. Thus, the mechanism for enhanced K emission must have little effect at 1.6 μm or at V. The most straightforward explanation is, again, warm dust. Telesco and Gatley (1984), for example, demonstrated the effects of a modest contribution from this thermal emission to near-infrared colors. Dust at temperatures less than several hundred degrees can make a small contribution to K band emission, but will make almost none at H, since the dust spectrum is dropping precipitously toward shorter wavelengths. Of course, modest emission from hot dust is also an attractive explanation in the arms and ring, where previous workers have established that star formation is extremely active.

b) The Mass of the Core Components

Central to understanding the dynamics and the evolution of the central region of NGC 1068 is determination of its stellar mass. Two techniques are commonly used to estimate this value: using the observed velocity of material in orbit or adopting a mass-to-light ratio. The former technique requires knowledge about the orientation of the galaxy, a reliable velocity, and an assumption about the mass distribution. Alternatively, adopting a mass-to-light ratio requires knowledge about the stellar population (e.g., age, mass function) that dominates the emission. We shall use the latter method here, but note that we do not have sufficient information about the stellar population to accomplish more than to put an upper limit on the mass near the center of NGC 1068. For example, Thronson and Greenhouse (1988) used the local solar neighborhood as a model for the stellar product of a long period of nearly constant star formation and found for this case

$$M_*(M_\odot) \approx 2.6 \times 10^8 D^2(\mathrm{Mpc}) F_K(\mathrm{Jy}) . \quad (1)$$

This formulation produced stellar masses in close agreement with those determined from rotation line surveys of a large variety of more-or-less normal galaxies (Devereux, Becklin, and Scoville 1987), including active star-forming galaxies such as NGC 253 and IC 342. Thronson and Greenhouse concluded that the reason for the wide applicability of equation (1) is, first, the initial mass function of newly formed stars is similar over a wide range of conditions in galaxies and, second, young stars normally add only a small fraction to the near-infrared light from the old stellar population. For the disk and bar of NGC 1068, we concluded (§ III*a*(ii)) that very young stars and hot dust make only a small contribution to the total light at K and H. However, if a large fraction of the stars contributing to the near-infrared light were born less than a few billion years ago, higher mass carbon and AGB stars will dominate the emission (Persson *et al.* 1983; Chokshi and Wright 1987) and any estimate made using equation (1) will be an upper limit.

Using our K image (Fig. 2*b*), we estimate $F_K \approx 1.2$ Jy from the stars in the bar/disk region of NGC 1068 (roughly the inner 50″ diameter region). This flux density does not include the Seyfert nucleus and assumes a 20% contribution from hot dust to the K light. From equation (1), we find $M_* \leq 10 \times 10^{10}\ M_\odot$ for the core of NGC 1068, where the upper limit is a consequence of our belief that many of the stars in this region may have been born less than a few times 10^9 yr ago and insufficient time has passed for the near-infrared light to be dominated by low-mass giants. Our result is about a factor of 4 greater than the mass of $2.6 \times 10^{10}\ M_\odot$ determined by Burbidge, Burbidge, and Prendergast (1959) in an extensive analysis of the circumnuclear velocity structure within this galaxy.

More recently, Scoville *et al.* (1988), in their study of the near-infrared core of the galaxy, used the velocity of the molecular material, an estimated inclination, and derived $M_* = 1.3 \times 10^{10}\ M_\odot$ within 16″ (1.4 kpc) of the nucleus. Over this region, our near-infrared data and the formula in equation (1) gives $M_* \leq 8 \times 10^{10}\ M_\odot$. Baldwin, Wilson, and Whittle (1987), in a detailed analysis of ionized gas motion in the galaxy, derived a circular rotation velocity of a factor of 1.5–2.5 times greater than that adopted by Scoville *et al.* (1988). This disagreement is due largely to the different adopted inclination angle of the galaxy: Baldwin, Wilson, and Whittle derive $i \approx 20°$–$35°$, while Scoville *et al.* adopted $i = 40°$, at the high end of estimated values for the inclination (see also Telesco and Decher 1988). Lower values of i lead to higher calculated circular velocities and, hence, a higher mass since $M_* \propto V_{\mathrm{circ}}^2$. If the actual inclination of the galaxy is 30°, which is the middle o'

the wide range proposed for NGC 1068, the data used by Scoville *et al.* would result in a mass interior to a radius of 1.4 kpc of $M_* \approx 2 \times 10^{10}\ M_\odot$, close to the determination by Burbidge, Burbidge, and Prendergast.

c) Star Formation in the Circumnuclear Core of NGC 1068

In this section, we calculate the rate and efficiency of star formation in the central few kiloparsecs of NGC 1068, compare the mass of gas and newly formed stars with that of the bar and surrounding disk, and estimate the lifetime of the star-forming material. In the following analysis, we wish to determine whether the high rate of stellar creation is a consequence of the large amount of molecular material or, instead, to a high efficiency of star birth. We shall conclude that the enormous rate of star formation in the circumnuclear core of the galaxy is a direct consequence of the very large molecular mass, presumably confined by the bar. Furthermore, we find that the efficiency of star formation is not particularly high in the core of NGC 1068.

Thronson and Telesco (1986) derived a formula relating total infrared emission to the rate of star formation,

$$\dot{M}(M_\odot\ \mathrm{yr}^{-1}) = 6.5 \times 10^{-10} L_{\mathrm{IR}}(L_\odot)\,, \qquad (2)$$

under the explicit assumption that very young stars are the sole source of heating for the grains. Application of this formula is uncertain in more bizarre objects, such as the core of NGC 1068 perhaps, since Thronson and Telesco assumed a normal Salpeter initial mass function (IMF) extending between 0.1 and 100 $M_\odot$ to derive this equation. Although roughly appropriate to many star-forming regions, numerous individuals have questioned the universality of both a wide range of stellar masses being formed and the Salpeter function. At present, "bimodal" and "truncated" IMFs are fashionable. However, Scalo (1987) surveyed arguments favoring such abnormal functions and concluded that their observational support was weak or nonexistent. From mid- and far-infrared observations (Telesco *et al.* 1984; Lester *et al.* 1987), the total infrared luminosity of the inner $\sim 2'$ diameter region of NGC 1068, excluding the luminous Seyfert nucleus, is about $1.5 \times 10^{11}\ L_\odot$, indicating a star-formation rate of $\sim 100\ M_\odot\ \mathrm{yr}^{-1}$. Telesco and Decher derived a similar value, within the uncertainties. Young, Kleinmann, and Allen (1988) used visual line data to derive a consistent value, but one that is lower by about a factor of 3 since these authors attempted to estimate only the *massive* star-formation rate. Based on the visual, mid-infrared, and CO maps, as discussed in the preceding section, star formation is taking place primarily in the ring that surrounds the bar/disk region, with a lower rate in the bar and disk.

Our near-infrared observations allow us to qualify the preceding discussion by accounting for the effect of heating of the dust grains by the general interstellar radiation field produced by the older stellar population. In a recent paper (Descartes *et al.* 1989), we discussed how near-infrared photometry can be used to estimate the total luminosity of an older stellar population. In particular, we proposed for a normal population of stars in the cores of spirals, $M_{\mathrm{bol}} \approx M_K + 2.0$. For the inner $\sim 1'$ diameter core of NGC 1068, $M_{\mathrm{bol}} \approx -22.4$, excluding the Seyfert nucleus and a 20% contribution from warm dust. For $M_{\mathrm{bol},\odot} = 4.75$, the stellar luminosity is $7 \times 10^{10}\ L_\odot$. This value is close to the far-infrared luminosity of the same region, again excluding the Seyfert nucleus, which suggests that the older stellar population plays an important role in heating the dust observed at far-infrared wavelengths. Unfortunately, as Descartes *et al.* discuss in detail, estimating the bolometric luminosity for nearly normal galaxies from near-infrared photometry is uncertain by at least a factor of 2 ... and NGC 1068 is far from normal. At present, we believe that we can only comment that the far-infrared luminosity derived for the star-forming region of this galaxy may include an important contribution from the older stellar population.

Thronson and Telesco (1986) also calculated that, for the IMF and its limits that they adopted, the mass-to-luminosity ratio for newly formed stars is $1.3 \times 10^{-3}\ M_\odot\ L_\odot^{-1}$. Assuming again that the far-infrared luminosity arises from young stars alone, the stellar mass is consequently about $2 \times 10^8\ M_\odot$, most of which lies in the star-forming ring investigated by Telesco and Decher (1988). Estimates of the molecular mass in the inner $\sim 2'$ of NGC 1068 vary over about a factor of 2 (Scoville, Young, and Lucy 1983; Myers and Scoville 1987; Thronson *et al.* 1987), but $7 \times 10^9\ M_\odot$ is a typical value. Hence, for the core of NGC 1068, $L_{\mathrm{IR}}/M(\mathrm{H}_2) \approx 21\ L_\odot\ M_\odot^{-1}$, with about a factor-of-2 uncertainty if the CO line flux and the millimeter continuum emission reliably measure the molecular mass. Furthermore, the mass of new stars divided by the molecular mass, which we interpret as the *instantaneous* star-formation efficiency, is about 0.03. Bearing in mind the high systematic uncertainty in this value, this is a very modest efficiency. Similarly, the value of $L_{\mathrm{IR}}/M(\mathrm{H}_2)$ for the core of NGC 1068 is only slightly larger than that derived for more-or-less normal spiral galaxies (e.g., Young *et al.* 1986; Thronson *et al.* 1987), although much of the earlier analysis of the infrared emission assumed (incorrectly, as we have emphasized above) that the sole source of dust heating is newly formed stars. We, nevertheless, conclude that the enormous observed infrared luminosity outside the Seyfert nucleus in NGC 1068 is likely to be primarily the product of a very high rate of star formation which, in turn, is a consequence of the accumulation of large amounts of molecular material by a vigorous stellar bar.

The fractional molecular gas mass in the inner 2′ diameter core of the galaxy is in the range 0.1–0.2, depending upon the adopted value for the gas mass and the reliability (or lack of it) in stellar mass determinations (previous section). The molecular gas can last only 10^8 yr at a star-formation rate of $100\ M_\odot\ \mathrm{yr}^{-1}$ if long-term star-formation is perfectly efficient, although we expect the star-formation rate to decrease as the gas is depleted.

It may be possible to test our estimated rate of star formation, by regularly searching for near-infrared or radio continuum emission from supernovae in the central few arcminutes of this galaxy. Thronson and Greenhouse (1988) related the star formation and supernova rates as $R_{\mathrm{SN}}\ (\mathrm{yr}^{-1}) \approx 0.006\ R_{\mathrm{SF}}\ (M_\odot\ \mathrm{yr}^{-1})$. We predict a supernova once every few years in the star-forming region of NGC 1068.

IV. SUMMARY

We have presented and discussed H (1.6 μm) and K (2.2 μm) images of the central $\sim 2'$ of the luminous Seyfert 2 galaxy NGC 1068 (M77). A major observational result is the revelation of the details of a strong barlike structure that must dominate the mass distribution and dynamics of the center of this galaxy. The bar apparently organizes the interstellar gas into a pair of truncated spiral arms, within which most of the current star formation is taking place. We also discuss the near-infrared emission from a disk within which the bar is embedded and from spiral arm features that appear to emerge from the star-forming ring that surrounds the core. Based on

models of the color of composite stellar systems, we conclude that the majority of the emission from the bar and disk arises from stars, although 10%–20% of the K emission may arise from hot dust. Thermal emission from star-forming regions also appears to trace the ring and spiral arm structure in $V-K$ and $H-K$ images.

It is possible that dust obscuration hides the bar from view at visual wavelengths, but near-infrared light from evolved stars easily penetrates this veil. Alternatively, we argue that it is possible that the stellar population in the bar and in the surrounding disk is different enough to cause the bar to merge with the disk at visual wavelengths, but be revealed at H and K. Either would explain the unusual situation of a strong bar that is revealed only at longer wavelengths.

We estimate the mass of stars in the bar and disk to be $2–3 \times 10^{10}\ M_{\odot}$. The molecular mass in the central 2.5 kpc of the galaxy is, therefore, about 10%–20% of the total, but is confined to the region of the core that is outside the bar/disk region. Star formation at present in the core NGC 1068 is also taking place primarily in this ring. There the rate of stellar creation is $\sim 100\ M_{\odot}\ \mathrm{yr}^{-1}$, which we conclude is due primarily to the large amount of molecular material, not to a particularly efficient process of star birth.

We appreciate conversations with, and data in advance of publication from, Greg Bothun, Rob Kennicutt, Nick Scoville, Charlie Telesco, and Judy Young. We are especially grateful to Charlie, who convinced us to move NGC 1068 higher in our priority list of galaxies to observe with our infrared camera. We appreciate the generosity of Rudy Schild in making his V-band data available to us. This work was supported by the NSF EPSCoR program grant number RII 8610680 and the Astrophysical Research Consortium.

REFERENCES

Aaronson, M. 1978, *Ap. J. (Letters)*, **221**, L103.
Alloin, D., Larques, P., Pelat, D., and Despiau, R. 1981, *Astr. Ap. Suppl.*, **43**, 231.
Antonucci, R. R. J., and Miller, J. S. 1985, *Ap. J.*, **297**, 621.
Atherton, P. D., Reay, N. K., and Taylor, K. 1985, *M.N.R.A.S.*, **216**, 17P.
Baldwin, J. A., Wilson, A. S., and Whittle, M. 1987, *Ap. J.*, **319**, 84.
Balick, B., and Heckman, T. M. 1985, *A.J.*, **90**, 197.
Burbidge, G. R. 1970, *Ann. Rev. Astr. Ap.*, **8**, 369.
Burbidge, E. M., Burbidge, G. R., and Prendergast, K. H. 1959, *Ap. J.*, **130**, 26.
Campbell, W. W., and Moore, J. H. 1918, *Lick Obs. Pub.*, **13**, 88.
Chokshi, A., and Wright, E. L. 1987, *Ap. J.*, **319**, 44.
Code, A. D. 1959, *Pub. A.S.P.*, **71**, 118.
Descartes, L., Thronson, H. A., Hereld, M., and Majewski, S. 1989, *Ap. J.*, submitted.
Devereux, N. A., Becklin, E. E., and Scoville, N. Z. 1987, *Ap. J.*, **312**, 529.
Elmegreen, B. G., and Elmegreen, D. M. 1985, *Ap. J.*, **288**, 438.
Fath, E. A. 1909, *Lick Obs. Pub.*, **5**, 71.
Frogel, J. A. 1985, *Ap. J.*, **298**, 528.
Hackwell, J. A., and Schweizer, F. 1983, *Ap. J.*, **265**, 643.
Hall, D. N. B., Kleinmann, S. G., Scoville, N. Z., and Ridgway, S. T. 1981, *Ap. J.*, **248**, 898.
Hereld, M., Harper, D. A., and Pernic, R. 1989, in preparation.
Hodge, P. 1968, *A.J.*, **73**, 846.
Huntley, J. M. 1980, *Ap. J.*, **238**, 524.
Ichikawa, S., Okamura, S., Kaneko, N., Nishimura, M., and Toyama, K. 1987, *Pub. Astr. Soc. Japan*, **39**, 411.
Kaneko, N., *et al.* 1988, preprint.
Keel, W., and Weedman, D. W. 1978, *A.J.*, **83**, 1.
Lausten, S., Madsen, C., and West, R. M. 1987, *Exploring the Southern Sky* (Berlin: Springer), p. 27.
Lester, D. F., Joy, M., Harvey, P. M., Ellis, H. B., and Parmar, P. S. 1987, *Ap. J.*, **321**, 755.
McCarthy, D. W., Low, F. J., Kleinmann, S. G., and Gillett, F. C. 1982, *Ap. J. (Letters)*, **257**, L7.
Myers, S. T., and Scoville, N. Z. 1987, *Ap. J. (Letters)*, **312**, L39.
Osterbrock, D. E., and Parker, R. A. 1965, *Ap. J.*, **141**, 892.
Persson, S. E., *et al.* 1983, *Ap. J.*, **266**, 105.
Pogge, R. 1988, preprint.
Roberts, W. W., Huntley, J. M., and van Albada, G. D. 1979, *Ap. J.*, **233**, 67.
Sandage, A., and Tammann, G. 1981, *A Revised Shapley-Ames Catalog of Bright Galaxies* (Washington, DC: Carnegie Institution of Washington).
Scalo, J. 1987, in *Starbursts and Galaxy Evolution*, ed. T. X. Thuan, T. Montmerle, and J. Tran Thanh Van (Paris: Editions Frontieres), p. 445.
Schild, R., Tresch-Fienberg, R., and Huchra, J. 1985, *A.J.*, **90**, 441.
Schwarz, M. P. 1981, *Ap. J.*, **247**, 77.
Scoville, N. Z., Matthews, K., Carico, D. P., and Sanders, D. B. 1988, *Ap. J. (Letters)*, **327**, L61.
Scoville, N. Z., Young, J. S., and Lucy, L. B. 1983, *Ap. J.*, **270**, 443.
Sellwood, J. A. 1981, *Astr. Ap.*, **99**, 362.
Seyfert, C. K. 1943, *Ap. J.*, **97**, 28.
Slipher, V. M. 1917, *Lowell Obs. Bull.*, **3**, 59.
Struck-Marcell, C., and Tinsley, B. 1978, *Ap. J.*, **221**, 562.
Telesco, C. M., Becklin, E., Wynn-Williams, C. G., and Harper, D. A. 1984, *Ap. J.*, **282**, 427.
Telesco, C. M., and Decher, R. 1988, *Ap. J.*, **334**, 573.
Telesco, C. M., and Gatley, I. 1984, *Ap. J.*, **284**, 557.
Thronson, H. A., and Greenhouse, M. A. 1988, *Ap. J.*, **327**, 671.
Thronson, H. A., Hereld, M., and Sloan, G. 1989, *A.J.*, in press.
Thronson, H. A., and Telesco, C. M. 1986, *Ap. J.*, **311**, 98.
Thronson, H. A., Walker, C. E., Walker, C. M., and Maloney, P. 1987, *Ap. J.*, **318**, 645.
Thuan, T. X. 1985, *Ap. J.*, **299**, 881.
Tresch-Fienberg, R., *et al.* 1987, *Ap. J.*, **312**, 542.
Véron-Cetty, M.-P., and Véron, P. 1983, *Messenger*, **34**, 22.
Visvanathan, N., and Oke, J. B. 1968, *Ap. J. (Letters)*, **152**, L65.
Weedman, D. W., and Huenemoerder, D. P. 1985, *Ap. J.*, **291**, 72.
Wilson, A. S., and Ulvestad, J. S. 1982, *Ap. J.*, **263**, 576.
Young, J. S., Kleinmann, S. G., and Allen, L. E. 1988, *Ap. J. (Letters)*, **334**, L63.
Young, J. S., Schloerb, F. P., Kenney, J. D., and Lord, S. D. 1986, *Ap. J.*, **304**, 443.

M. GREENHOUSE, P. JOHNSON, E. SPILLAR, H. THRONSON, and C. WOODWARD: Wyoming Infrared Observatory, Box 3905, University of Wyoming, Laramie, WY 82071

D. A. HARPER, S. MAJEWSKI, and B. J. RAUSCHER: Yerkes Observatory, Box 258, Williams Bay, WI 53191

M. HERELD: Department of Astronomy and Astrophysics, University of Chicago, 5640 S. Ellis Avenue, Chicago, IL 60637